Journal of Thermal Analysis and Calorimetry (2018) 132:761–770
https://doi.org/10.1007/s10973-017-6881-4

A novel method for predicting decomposition onset temperature of cubic polyhedral oligomeric silsesquioxane derivatives

Kamal Ghani[1] · Mohammad Hossein Keshavarz[1] · Mohammad Jafari[1] · Fatemeh Khademian[1]

Received: 13 July 2017 / Accepted: 3 December 2017 / Published online: 12 December 2017

Abstract
A novel simple approach is introduced to predict the decomposition onset temperature of cubic polyhedral oligomeric silsesquioxane, POSS, compounds through their molecular structures. It is based on the number of organic groups attached to silicon atoms and some structural moieties that depend on the type and size of substituents. The present method can be easily applied for cubic POSS containing different substituents attached to silicon atom without using special computer codes, which need expert users. The measured data for 50 cubic POSS compounds are used to construct new model with good coefficient of determination (R^2), i.e., $R^2 = 0.9384$. Statistical parameters including the root-mean-squared error, mean absolute percent error and maximum of errors of the new model are 19.2, 4.6 and 66.5 K, respectively, which confirm high reliability of the new method. The method is tested for further four POSS compounds including complex molecular structures, which give good results. Cross-validation of models is also used to evaluate the goodness-of-fit, goodness-of-prediction, accuracy and precision of the new model.

Keywords Decomposition temperature · Cubic POSS · Molecular structure · Thermal stability

Introduction

Polyhedral oligomeric silsesquioxane (POSS) molecules are inorganic/organic hybrid cage-type nanostructures with the general formula of $(RSiO_{3/2})_n$, where n is 6, 8, 10, etc., and R can be hydrogen, alkyl, alkylene, aryl or other organofunctional derivatives. Due to the many useful applications, various research works have been done on POSS compounds in recent years [1]. Cubic POSS ($(RSiO_{3/2})_8$) compounds are especially important because they can be considered as starting materials for the synthesis of a wide range of materials with the desired properties [2, 3]. In octafunctional POSS compounds, the central inorganic core, Si_8O_{12}, is surrounded symmetrically by distribution of organic moieties. The composition of silsesquioxane containing inorganic core, Si_8O_{12}, and organic groups describes their thermal and mechanical properties. Moreover, the organic periphery on their silicon atom, which can be easily functionalized, allows a facile tuning of the silsesquioxane properties [1, 4]. Figure 1 shows the general structure of an octafunctional POSS compound.

Cubic POSS materials are widely used in various branches of material science such as catalysis [5–7], flame-resistant nanocomposites [8, 9], biomedicals [10, 11], light-emitting diode materials [12–14], ionic liquids [15], ionic crystals [16], electrolytes with high thermal stability [17] and functional coatings [18, 19]. Thermal stability is an important characteristic of POSS compounds, which improves the thermal properties of polymer nanocomposites and hybrids. Thermal analysis methods are used to investigate the thermal degradation of POSS materials. Thermal stability and decomposition of cubic POSS have been studied by the thermogravimetric analysis (TGA) [4, 10]. Different thermal analysis methods have been used widely for the evaluation of thermal stability [4, 10, 20–36]. The heat of decomposition shows a relatively large error of about 10%. Meanwhile, the exothermic onset temperature, the temperature at which the first deflection from the baseline is observed, thermal

✉ Mohammad Hossein Keshavarz
mhkeshavarz@mut-es.ac.ir; keshavarz7@gmail.com

[1] Department of Chemistry, Malek-ashtar University of Technology, Shahin-Shahr, P.O. Box 83145/115, Islamic Republic of Iran

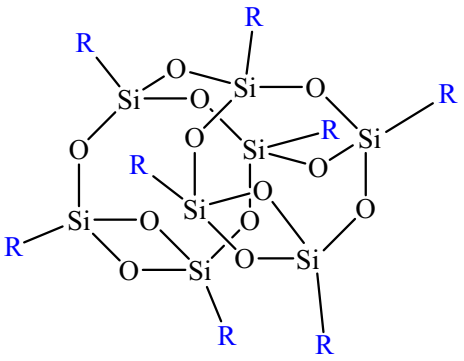

Fig. 1 General structure of a cubic POSS compound with the formula of $(RSiO_{3/2})_8$

decomposition temperature and the temperature at which maximum of mass loss give better reproducibility than that of the heat of decomposition. For classes of organic compounds containing energetic groups, there are some relationships between activation energy of thermolysis and the other stimuli for initiation of their decomposition [37, 38].

Development of suitable predictive methods on thermal stability parameters such as decomposition onset temperature can help the scientists to increase their knowledge on the synthesis of good candidate. Quantitative structure–property relationship (QSPR) studies are usually used for this purpose [39–45], but they require some complex molecular descriptors, e.g., constitutional and topological, as well as special computer codes, which need expert users. Some molecular moieties of the desired compounds can also be used to predict thermal stability parameters of classes of organic compounds [46]. Since molecular structure of a desired compound can be used to study its thermal analysis, the purpose of this paper is to introduce a novel simple model for evaluation of the decomposition onset temperature (T_{decom}) as important parameter for the assessment of thermal stability of cubic POSS compounds. It will be shown that there is no need for complex computer code and descriptors as well as expert users. The new model correlates T_{decom} to the molecular structure of POSS materials using several simple molecular descriptors.

Materials and methods

Experimental data of T_{decom} under N_2 for 54 cubic POSS compounds were collected from different sources. Among these compounds, 44 cubic POSS compounds containing simple or similar molecular fragments were used to construct the new model, which are given in Table 1. Ten cubic POSS compounds containing complex molecular moieties were also chosen to test the validity of the novel correlation.

Results and discussion

Development of the new model

The study of T_{decom} of different cubic POSS compounds has shown that it is possible to introduce a new correlation on the basis of the number of some specific atoms divided by molecular weight of POSS compound by considering the type and size of substituents without using complex molecular descriptors. It was found that the existence of several molecular fragments can increase or decrease the predicted T_{decom} on the basis of elemental composition by two correcting functions. The following correlation was derived on the basis of the measured values given in Table 1 by using multiple linear regression method ($R^2 = 0.9384$) [47]:

$$T_{decom} = 516.0 + 3.034 \times 10^4 \frac{n_C}{Mw} - 1.021 \times 10^4 \frac{n_H}{Mw} - 2.560 \times 10^4 \frac{n_O}{Mw} + 9.941 \times 10^4 \frac{n_{Cl}}{Mw} + 121.3T^{+}_{decom} - 108.3T^{-}_{decom} \quad (1)$$

where n_C, n_H, n_O and n_{Cl} are the number of carbon, hydrogen, oxygen and chlorine atoms in R (Fig. 1), respectively; T^{+}_{decom} and T^{-}_{decom} are two correcting functions, which are used to show increasing and decreasing the contribution of nonadditive structural parameters, respectively; Mw is the molecular weight of the desired POSS compound. To derive Eq. (1) by multiple linear regression method, several steps have been done to find the variables containing statistically significant. At first, various combination of elemental composition, functional groups and structural parameters have been tested. It was found that $\frac{n_C}{Mw}, \frac{n_H}{Mw}, \frac{n_O}{Mw}$ and $\frac{n_{Cl}}{Mw}$ and the presence of some substituents with specific molecular structures are important. Moreover, four variables $\frac{n_C}{Mw}, \frac{n_H}{Mw}, \frac{n_O}{Mw}$ and have significant contributions with respect to the other elements by evaluation of statistical parameters. Finally, the contribution of structural parameters has also been included by two terms and T^{-}_{decom} for increasing and decreasing T_{decom}. The study of T_{decom} for polynitro arenes has confirmed that the same trend exists for coefficients n_C, n_H and n_O [48]. As seen in Table 2, there is a direct dependency of and on the substituent type and size. For example, the values of T^{+}_{decom} and T^{-}_{decom} should be considered for phenyl and alkyl substituents under certain conditions, respectively, because the thermal behavior of phenyl substituents of POSS is completely different from those of alkyl substituted POSS.

Table 1 Predictions of Eq. (1) for the decomposition onset temperature of cubic POSS compounds, compared to the experimental data (training set)

No.	R	Experimental T_{decom}/K	Predicted T_{decom}/K	Dev.
1		373.2 [52]	383.7	10.6
2	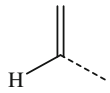	553.2 [1]	563.5	10.4
3	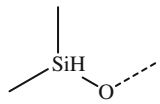	461.2 [53]	480.3	19.2
4	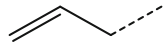	463.2 [53]	461.4	– 1.7
5	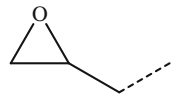	525.2 [53]	532.5	7.4
6	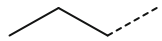	439.2 [54]	433.5	– 5.7
7	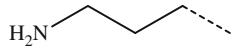	593.2 [1]	526.7	– 66.5
8	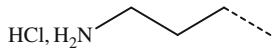	595.2 [55]	600.1	4.9
9	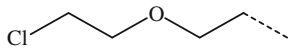	611.2 [56]	604.9	– 6.2
10	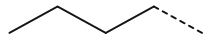	473.2 [54]	474.0	0.9
11	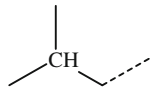	477.2 [1]	474.0	– 3.1
12	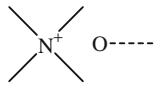	473.2 [57]	492.5	19.4
13	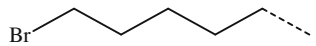	654.2 [56]	668.0	13.9
14		508.2 [54]	512.7	4.6
15	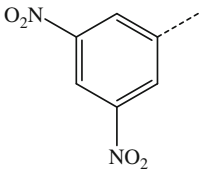	693.2 [1]	669.4	– 23.7
16	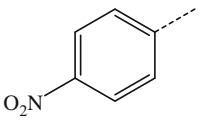	615.2 [58]	580.6	– 34.5
17	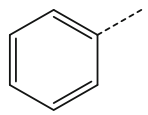	738.2 [59]	764.1	26.0
18	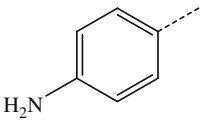	687.2 [58]	681.4	– 5.7

Table 1 continued

No.	R	Experimental T_{decom}/K	Predicted T_{decom}/K	Dev.
19	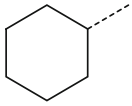	583.2 [1]	580.5	– 2.6
20	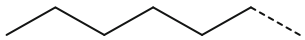	538.2 [54]	550.2	12.0
21	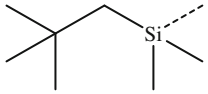	573.2 [60]	537.6	– 35.5
22	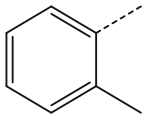	708.2 [59]	699.7	– 8.4
23	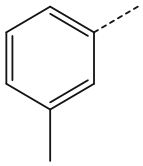	704.2 [59]	699.7	– 4.4
24	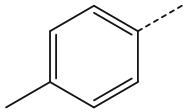	686.2 [59]	639.1	– 47.1
25	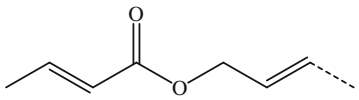	575.2 [1]	557.5	– 17.7
26	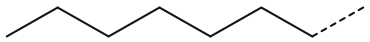	563.2 [54]	565.0	1.9
27	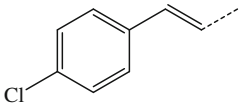	635.2 [61]	636.2	1.1
28	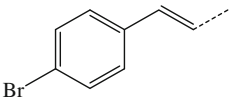	591.2 [61]	612.9	21.8
29	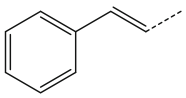	668.2 [61]	654.0	– 14.2
30	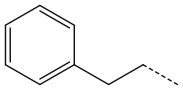	623.2 [1]	636.0	12.8
31	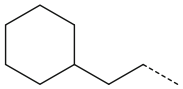	715.2 [56]	705.9	– 9.2
32		583.2 [54]	568.4	– 14.8
33	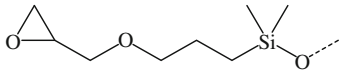	623.2 [1]	633.4	10.2
34	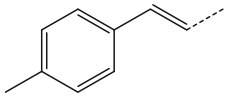	556.2 [1]	563.3	7.1

Table 1 continued

No.	R	Experimental T_{decom}/K	Predicted T_{decom}/K	Dev.
35	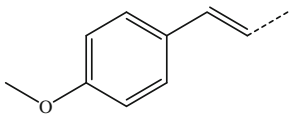	596.2 [1]	621.0	24.9
36		608.2 [54]	633.4	25.2
37	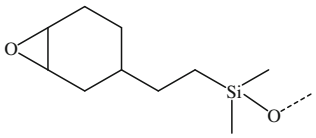	677.2 [1]	666.3	– 10.9
38	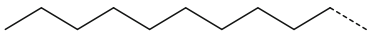	628.2 [54]	634.3	6.1
39	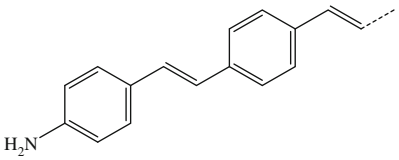	618.2 [61]	619.1	1.0
40	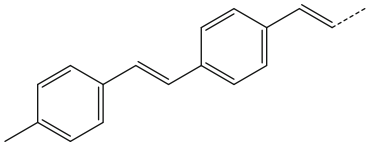	663.2 [61]	683.1	20.0
41	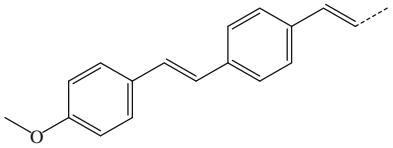	588.2 [61]	576.0	–12.1
42	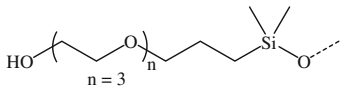	471.2 [62]	496.6	25.4
43	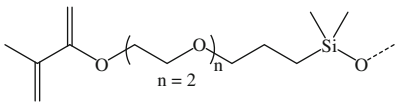	455.2 [62]	455.2	0.0
44	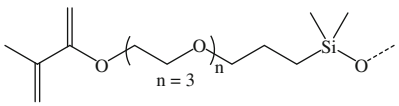	455.2 [62]	452.8	– 2.3

In fact, some phenyl substituents show considerably a higher high thermal stability. Since the collected data of T_{decom} are under nitrogen atmosphere, cleavage of weak bond in substituents is one of the important factor for the contribution of . Since the coefficients of $\frac{n_C}{Mw}$ and $\frac{n_{Cl}}{Mw}$ in Eq. (1) have positive sign, increment of the number of carbon and chlorine atoms can increase the value of T_{decom}. Meanwhile, decreasing the values of n_H and n_O can also increase the value of T_{decom}. There is no contribution for the other atoms in Eq. (1) because their contributions do not improve the value of the coefficient of determination (R^2). The values of T^+_{decom} and are given in Table 2 for different molecular fragments. They can adjust high deviations of the predicted T_{decom} only on the basis of $\frac{n_C}{Mw}, \frac{n_H}{Mw}, \frac{n_O}{Mw}$ and from experimental data. For those POSS compounds where the estimated results of T_{decom} from $\frac{n_C}{Mw}, \frac{n_H}{Mw}, \frac{n_O}{Mw}$ and show relatively large underestimated and overestimated predictions with respect to experimental data, respectively, the contributions T^+_{decom} and are valid. As seen in Table 2, direct attachment of aromatic rings, hydrogen atoms and saturated or unsaturated hydrocarbon under certain conditions as well as the presence of some

Table 2 Values of T^{+}_{decom} and T^{-}_{decom} for prediction of the onset decomposition temperature of $R_8(SiO_{1.5})_8$ Compounds

R	T^{+}_{decom}	T^{-}_{decom}
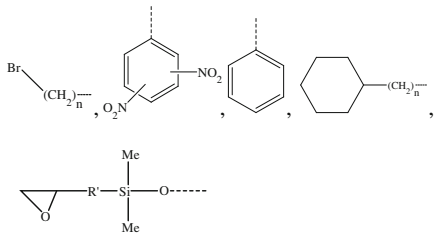 R' = substituents containing C,H,O atoms	1.0	0
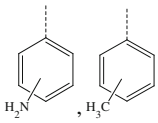	0.5	0
H-----	0	1.0
R----- R = saturated or unsaturated hydrocarbon	0	1.0–0.3(n – 3) , 3≤ n ≤6 n = number of carbon atom
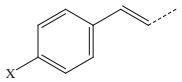	0	0.6 (X = Cl)
		0.8 (X = Alkyl)
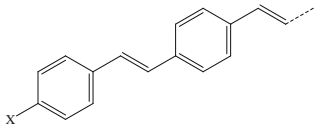	0	0.5 (X = NH_2)
		0.8 (X = –OR´)
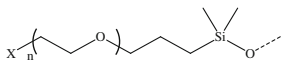	0	0.6 (X = –OOCR´)

specific functional groups to the central inorganic core are important parameters for taking the existence and different values for T^{+}_{decom} and . For those compounds where the conditions of either T^{+}_{decom} or given in Table 2 are not satisfied, their values in Eq. (1) are equal to zero. It should be mentioned that Eq. (1) can be applied only for POSS compounds containing eight similar substituents.

Statistical evaluation of the new model

Table 3 shows statistical parameters corresponding to variables given in Eq. (1). The values of standard deviation (SD) for variables indicate the significant of individual variables for estimation of the dependent variable. As seen in Table 3, the variables are significant because the values of SD of the variables are small relative to corresponding coefficients. The P value gives the probability that the observed results in a study could have occurred by chance. If the detected effect is not due to random variations for P value < 0.05, the effect will be significant. As indicated in Table 3, the results of P-value of four variables are less than 0.05, which confirm that they have a highly significant impact. Figure 2 shows the predicted T_{decom} using the developed model versus experimental values given in Table 1. Figure 3 also shows the range of the absolute percent errors of new model for these data.

Table 3 Regression coefficients of Eq. (1), as well as their standard deviations (SD), P values and confidence intervals

Descriptor	Coefficients	SD	P value	Lower bound (95%)	Upper bound (95%)
Intercept	516.0	14.8	3.560×10^{-35}	486.2	545.9
$\frac{n_C}{Mw}$	3.034×10^{4}	2.276×10^{3}	1.379×10^{-17}	2.577×10^{4}	3.492×10^{4}
$\frac{n_H}{Mw}$	-1.021×10^{4}	1.161×10^{3}	1.722×10^{-11}	-1.254×10^{4}	-7.873×10^{3}
$\frac{n_O}{Mw}$	-2.560×10^{4}	4.004×10^{3}	6.797×10^{-8}	-3.366×10^{4}	-1.755×10^{4}
$\frac{n_{Cl}}{Mw}$	9.941×10^{4}	1.875×10^{4}	2.995×10^{-6}	6.170×10^{4}	1.371×10^{5}
T^{+}_{decom}	121.3	10.07	5.658×10^{-16}	101.0	141.5
T^{-}_{decom}	− 108.3	10.23	4.969×10^{-14}	− 128.9	− 87.70

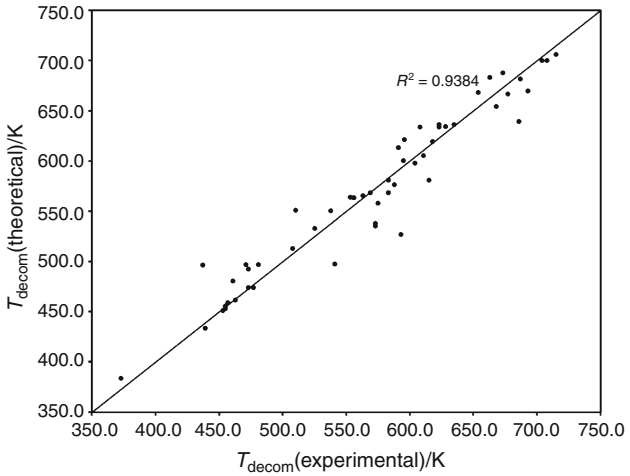

Fig. 2 Predicted T_{decom}/K using the developed model versus experimental values for training set

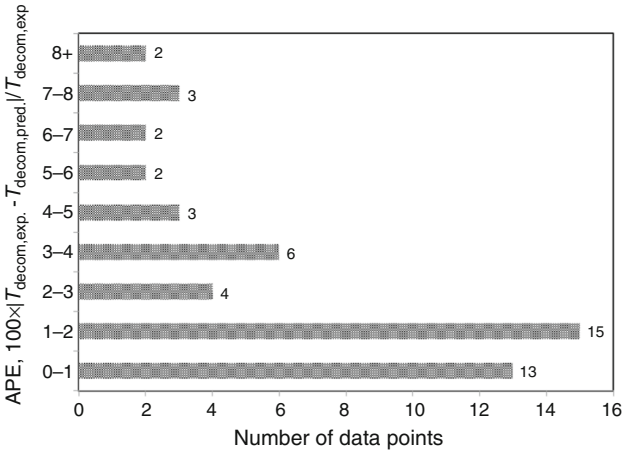

Fig. 3 Range of the absolute percent errors of new model for training set

Table 4 shows reliability of Eq. (1) method for several further POSS compounds containing complex molecular structures. As seen in Table 4, the predicted results are also close to the measured data. Table 5 indicates statistical parameters of the new model in cross-validation. Goodness-of-prediction is measured by Q^2 where Q^2 is smaller than R^2 but if the model is well behaved, there should not be a significant difference between Q^2 and R^2 [49] and in a robust model the Q^2 is independent of partition size and also close to R^2 [50]. For a suitable QSPR model, its R^2 is greater than 0.6 and its Q^2 values are greater than 0.5 [51]. As seen in Table 5, the coefficient of determination for LOO-CV (Q^2_{LOO}) of Eq. (1) is 0.9189. Meanwhile, the fivefold CV (Q^2_{5CV}), which is the average of 100 runs, is 0.8812. Both Q^2_{LOO} and Q^2_{5CV} are smaller than R^2. Since all values of R^2, Q^2_{LOO}, and Q^2_{5CV} are significantly greater than the threshold values, i.e., 0.6 for R^2 and 0.5 for Q^2, respectively, Eq. (1) is a reliable predictive QSPR model. Since both the Q^2_{LOO} and Q^2_{5CV} values are close to the R^2, the new model is robust, well behaved and more importantly, not over-fitted model. The mean absolute percent error (MAPE) and root-mean-squared error (RMSE) values and for LOO-CV and fivefold CV of Eq. (1) are close to the MAPE and RMSE of Eq. (1). Table 6 compares some statistical parameters for training and test sets. As seen, RMSE, MAPE and maximum error (Max Error) for test set is lower than training set, which indicates that external validation test for four further POSS compounds containing complex molecular structures is good.

Conclusions

This work introduces a novel method for prediction of T_{decom} of different POSS compounds. As indicated in Eq. (1), the novel model requires the values of $\frac{n_C}{Mw}$, $\frac{n_H}{Mw}$, $\frac{n_O}{Mw}$ and as well as two correcting functions T^{+}_{decom} and . The new method is a very simple model because there is no need to use computer codes and complex molecular descriptors. Equation (1) can explain important structural parameters to have the desired values of T_{decom} for a new designed POSS compound. In contrast to the other QSPR methods, Eq. (1) gives the simplest and reliable method for

Table 4 Predictions of Eq. (1) for the decomposition onset temperature of cubic POSS compounds, compared to the experimental data (test set)

No.	R	Experimental T_{decom}/K	Predicted T_{decom}/K	Dev.
1	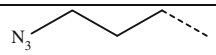	510.2 [1]	550.5	40.3
2	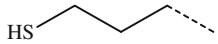	573.2 [1]	535.3	– 37.9
3	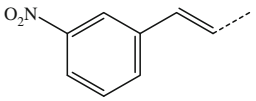	604.2 [1]	597.4	– 6.8
4	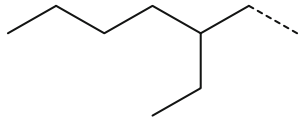	569.2 [54]	568.4	– 0.8
5	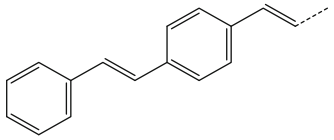	673.2 [61]	687.4	14.2
6	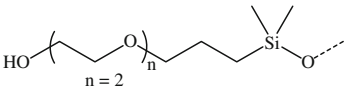	437.2 [62]	496.1	58.9
7	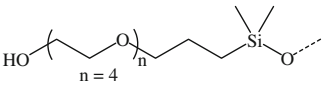	481.2 [62]	497.0	15.8
8	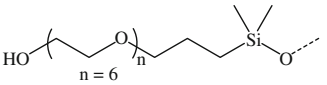	541.2 [62]	497.5	– 43.7
9	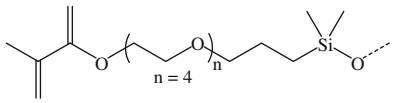	453.2 [62]	451.0	– 2.2
10	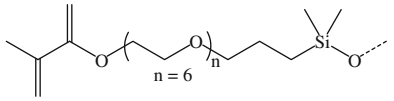	457.2 [62]	459.1	1.9

Table 5 Statistical parameters of the new model in cross-validation

Parameter	Whole model	Cross-validation	
		Leave-one-out	Fivefold[a]
Coefficients of determination	0.9384[b]	0.9189[c]	0.8812[d]
MAPE	4.6[e]	3.1[f]	3.2[g]
RMSE	19.2[h]	24.4[i]	22.9[j]

[a]For 100 runs; [b]R^2; [c]Q^2_{LOO}; [d]Q^2_{5CV}; [e]$MAPE_{Model}$; [f]$MAPE_{LOO}$; [g]$MAPE_{5CV}$; [h]$RMSE_{Model}$; [i]$RMSE_{LOO}$; [j]$RMSE_{5CV}$

Table 6 Statistical parameters of the new model in external validation

Data set	Datapoints	RMSE	MAPE	Max error	R^2	F statistic	Significance F
Training set	44	19.2	4.6	66.5	0.9384	119.230	1.01×10^{-26}
Test set	10	29.9	9.8	58.9	–	–	–

calculation of T_{decom} of different POSS compounds with good heat safety.

Acknowledgements We would like to thank the research committee of Iran University of Science and Technology for supporting this work.

References

1. Cordes DB, Lickiss PD, Rataboul F. Recent developments in the chemistry of cubic polyhedral oligosilsesquioxanes. Chem Rev. 2010;110(4):2081–173.
2. Eaton PE. Cubanes: starting materials for the chemistry of the 1990s and the new century. Angew Chem Inf Ed Engl. 1992;31:1421–36.
3. Roll MF, Asuncion MZ, Kampf J, Laine RM. Para-Octaiodophenylsilsesquioxane,[p-IC6H4SiO1.5]8, a nearly perfect nano-building block. ACS Nano. 2008;2:320–6.
4. Hartmann-Thompson C. Applications of polyhedral oligomeric silsesquioxanes. Berlin: Springer; 2011.
5. Levitsky MM, Yalymov AI, Kulakova AN, Petrov AA, Bilyachenko AN. Cage-like metallasilsesquioxanes in catalysis: a review. J Mol Catal A Chem. 2017;426:297–304.
6. Leng Y, Liu J, Zhang C, Jiang P. A polyhedral oligomeric silsesquioxane (POSS)-bridged oxo-molybdenum Schiff base complex with enhanced heterogeneous catalytic activity in epoxidation. Catal Sci Technol. 2014;4(4):997–1004.
7. Bivona LA, Fichera O, Fusaro L, Giacalone F, Buaki-Sogo M, Gruttadauria M, et al. A polyhedral oligomeric silsesquioxane-based catalyst for the efficient synthesis of cyclic carbonates. Catal Sci Technol. 2015;5(11):5000–7.
8. Raftopoulos KN, Pielichowski K. Segmental dynamics in hybrid polymer/POSS nanomaterials. Prog Polym Sci. 2016;52:136–87.
9. Tang Y, Lewin M. Migration and surface modification in polypropylene (PP)/polyhedral oligomeric silsequioxane (POSS) nanocomposites. Polym Adv Technol. 2009;20:1–15.
10. Tanaka K, Chujo Y. Advanced functional materials based on polyhedral oligomeric silsesquioxane (POSS). J Mater Chem. 2012;22:1733–46.
11. Wu J, Mather PT. POSS polymers: physical properties and biomaterials applications. J Macromol Sci Pol R. 2009;49:25–63.
12. Chan KL, Sonar P, Sellinger A. Cubic silsesquioxanes for use in solution processable organic light emitting diodes (OLED). J Mater Chem. 2009;19:9103–20.
13. Irie Y, Naka K. Single component transparent free-standing films based on polyhedral octasilicate-core dendrimers bearing carbazole terminal groups and their emission properties. J Polym Sci A. 2016;1(54):628–33.
14. Ren Z, Yan S. Polysiloxanes for optoelectronic applications. Prog Mater Sci. 2016;83:383–416.
15. Jeon J-H, Tanaka K, Chujo Y. Synthesis of sulfonic acid-containing POSS and its filler effects for enhancing thermal stabilities and lowering melting temperatures of ionic liquids. J Mater Chem A. 2014;2:624–30.
16. Kim N, Kim D-Y, Park M, Choi Y-J, Kim S, Lee SH, et al. Asymmetric organic–inorganic hybrid giant molecule: hierarchical smectic phase induced from POSS nanoparticles by addition of nematic liquid crystals. J Phys Chem C. 2014;119:766–74.
17. Chinnam PR, Wunder SL. Polyoctahedral silsesquioxane-nanoparticle electrolytes for lithium batteries: POSS-lithium salts and POSS-PEGs. Chem Mater. 2011;23:5111–21.
18. Rakesh S, Dharan CS, Selladurai M, Sudha V, Sundararajan P, Sarojadevi M. Thermal and mechanical properties of POSS-Cyanate ester/epoxy nanocomposites. High Perform Polym. 2013;25(1):87–96.
19. Minton TK, Wright ME, Tomczak SJ, Marquez SA, Shen L, Brunsvold AL, et al. Atomic oxygen effects on POSS polyimides in low earth orbit. ACS Appl Mater Interfaces. 2012;4:492–502.
20. Liu Y, Jiang Y-T, Zhang T-L, Feng C-G, Yang L. Thermal kinetic performance and storage life analysis of a series of high-energy and green energetic materials. J Therm Anal Calorim. 2015;119(1):659–70.
21. Kazemi A, Hayaty M, Mousaviazar A, Samani KA, Keshavarz MH. The synthesis and characterization of polyvinyl nitrate as an energetic polymer and study of its thermal behavior. J Therm Anal Calorim. 2015;119(1):613–8.
22. Huang H, Shi Y, Yang J. Thermal characterization of the promising energetic material TKX-50. J Therm Anal Calorim. 2015;121(2):705–9.
23. Singh CP, Singh A, Daniliuc CG, Kumar B, Singh G. Preparation, crystal structure and thermal studies of cadmium perchlorate complex with 2,2′-bipyridine. J Therm Anal Calorim. 2015;121(2):633–40.
24. Zhang G, Zhang J, Wang F, Li H. Thermal decomposition and kinetics studies on the poly (2,2-dinitropropyl acrylate) and 2,2-dinitropropyl acrylate–2, 2-dinitrobutyl acrylate copolymer. J Therm Anal Calorim. 2015;122(1):419–26.
25. Singh S, Singh G, Kulkarni N, Mathe V, Bhoraskar S. Synthesis, characterization and catalytic activity of Al/Fe_2O_3 nanothermite. J Therm Anal Calorim. 2015;119(1):309–17.
26. Izato Y, Miyake A. Thermal decomposition mechanism of ammonium nitrate and potassium chloride mixtures. J Therm Anal Calorim. 2015;121(1):287–94.
27. Wang X-J, You J-Z. Study on the molecular structure and thermal stability of pyrimidine nucleoside analogs. J Therm Anal Calorim. 2015;120(1):1009–25.
28. Keshavarz MH, Bashavard B, Goshadro A, Dehghan Z, Jafari M. Prediction of heats of sublimation of energetic compounds using their molecular structures. J Therm Anal Calorim. 2015;120(3):1941–51.
29. Keshavarz MH, Ghani K, Asgari A. A suitable computer code for prediction of sublimation energy and deflagration temperature of energetic materials. J Therm Anal Calorim. 2015;121(2):675–81.
30. Keshavarz MH. A new computer code for prediction of enthalpy of fusion and melting point of energetic materials. Propellants Explos Pyrotech. 2015;40(1):150–5.
31. Zohari N, Keshavarz MH, Dalaei Z. Prediction of decomposition onset temperature and heat of decomposition of organic peroxides using simple approaches. J Therm Anal Calorim. 2016;125(2):887–96.
32. Keshavarz MH, Pouretedal HR, Saberi E. A new method for predicting decomposition temperature of imidazolium-based energetic ionic liquids. Zeitschrift für anorganische und allgemeine Chemie. 2017;643(2):171–9.
33. Mousaviazar A, Keshavarz MH, Hayaty M, Kazemi A. Synthesis, characterization and thermal behavior of 2,4-dinitrophenoxy ethanol as a suitable plasticizer for propellants formulations. J Therm Anal Calorim. 2016;126(2):681–8.
34. Keshavarz MH, Esmaeilpour K, Taghizadeh H. A new approach for assessment of glass transition temperature of acrylic and methacrylic polymers from structure of their monomers without using any computer codes. J Therm Anal Calorim. 2016;126(3):1787–96.
35. Keshavarz MH, Mousaviazar A, Hayaty M. A novel approach for assessment of thermal stability of organic azides through prediction of their temperature of maximum mass loss. J Therm Anal Calorim. 2017;129(3):1659–65.

36. Mousaviazar A, Keshavarz MH, Hayaty M. The effect of cellulose derivatives on the phase transition and thermal behavior of ammonium nitrate. J Therm Anal Calorim. 2017;128(2):1049–56.
37. Keshavarz MH, Zohari N, Seyedsadjadi SA. Validation of improved simple method for prediction of activation energy of the thermal decomposition of energetic compounds. J Therm Anal Calorim. 2013;114(2):497–510.
38. Keshavarz MH, Zohari N, Seyedsadjadi SA. Relationship between electric spark sensitivity and activation energy of the thermal decomposition of nitramines for safety measures in industrial processes. J Loss Prev Process Ind. 2013;26(6):1452–6.
39. Fayet G, Rotureau P, Adamo C. On the development of QSPR models for regulatory frameworks: the heat of decomposition of nitroaromatics as a test case. J Loss Prev Process Ind. 2013;26(6):1100–5.
40. Wang B, Yi H, Xu K, Wang Q. Prediction of the self-accelerating decomposition temperature of organic peroxides using QSPR models. J Therm Anal Calorim. 2017;128(1):399–406.
41. Zohari N, Abrishami F, Sheibani N. A novel simple correlation for predicting glass transition temperature of energetic azido-ester plasticizers through molecular structures. J Therm Anal Calorim. 2017;127(3):2243–51.
42. Keshavarz MH, Dashtizadeh A, Motamedoshariati H, Soury H. A simple model for reliable prediction of the specific heat release capacity of polymers as an important characteristic of their flammability. J Therm Anal Calorim. 2017;128(1):417–26.
43. Mathieu D, Alaime T, Beaufrez J. From theoretical energy barriers to decomposition temperatures of organic peroxides. J Therm Anal Calorim. 2017;129(1):323–37.
44. Keshavarz MH, Esmaeilpour K, Saani MH, Taghizadeh H. A new method for assessment of glass transition temperature of ionic liquids from structure of their cations and anions without using any computer codes. J Therm Anal Calorim. 2017;130(3):2369–87.
45. Yu X, Huang L. Prediction of the onset temperature of decomposition of lubricant additives. J Therm Anal Calorim. 2017. https://doi.org/10.1007/s10973-017-6511-1.
46. Keshavarz MH, Ghani K, Asgari A. A new method for predicting heats of decomposition of nitroaromatics. Zeitschrift für anorganische und allgemeine Chemie. 2015;641(10):1818–23.
47. Palm WJ. Introduction to MATLAB 7 for engineers. 3rd ed. New York: McGraw-Hill; 2010.
48. Keshavarz M, Pouretedal H, Semnani A. Relationship between thermal stability and molecular structure of polynitro arenes. Indian J Eng Mater Sci. 2009;16:61–4.
49. Leach AR, Gillet VJ. An introduction to chemoinformatics. The Netherlands: Springer; 2007.
50. Fayet G, Rotureau P. Development of simple QSPR models for the impact sensitivity of nitramines. J Loss Preven Proc. 2014;30:1–8.
51. Tropsha A. Best practices for QSAR model development, validation, and exploitation. Mol Inf. 2010;29:476–88.
52. Nie WY, Li G, Li Y, Xu HY. Preparation and properties of a POSS-containing organic–inorganic hybrid crosslinked polymer. Chin Chem Lett. 2009;20(6):738–42.
53. Lee L-H, Chen W-C. Organic–inorganic hybrid materials from a new octa (2,3-epoxypropyl) silsesquioxane with diamines. Polymer. 2005;46(7):2163–74.
54. Bolln C, Tsuchida A, Frey H, Mülhaupt R. Thermal properties of the homologous series of 8-fold alkyl-substituted octasilsesquioxanes. Chem Mater. 1997;9(6):1475–9.
55. Liu L, Hu Y, Song L, Chen H, Nazare S, Hull TR. Lamellar hybrid from octa (γ-chloroaminopropyl) polyhedral oligomeric silsesquioxanes and anionic surfactant by ion-exchange reaction. Mater Lett. 2007;61(4):1077–81.
56. Dare EO, Olatunji GA, Ogunniyi DS. Organic–inorganic hybrid material. I. Synthesis, characterization, and thermal property of a novel polyhedral cubic silsesquioxane. J Appl Polym Sci. 2004;93(2):907–10.
57. Liu L, Hu Y, Song L, Nazare S, He S, Hull R. Combustion and thermal properties of OctaTMA-POSS/PS composites. J Mater Sci. 2007;42(12):4325–33.
58. Fan H, Yang R. Thermal decomposition of polyhedral oligomeric octaphenyl, octa (nitrophenyl), and octa (aminophenyl) silsesquioxanes. J Therm Anal Calorim. 2014;116(1):349–57.
59. Pakjamsai C, Kawakami Y. Study on effective synthesis and properties of ortho-alkyl-substituted phenyl octasilsesquioxane. Des Monomers Polym. 2005;8(5):423–35.
60. Unno M, Matsumoto T, Mochizuki K, Higuchi K, Goto M, Matsumoto H. Structure and oxidation of octakis (tert-butyldimethylsilyl) octasilacubane. J Organomet Chem. 2003;685(1):156–61.
61. Sulaiman S, Bhaskar A, Zhang J, Guda R, Goodson Iii T, Laine RM. Molecules with perfect cubic symmetry as nanobuilding blocks for 3-D assemblies. Elaboration of octavinylsilsesquioxane. Unusual luminescence shifts may indicate extended conjugation involving the silsesquioxane core. Chem Mater. 2008;20(17):5563–73.
62. Lee Y-J, Huang J-M, Kuo S-W, Lu J-S, Chang F-C. Polyimide and polyhedral oligomeric silsesquioxane nanocomposites for low-dielectric applications. Polymer. 2005;46(1):173–81.